Distribution of fixed beneficial mutations and the rate of adaptation in asexual populations

Benjamin H. Good[a,b,c], Igor M. Rouzine[d,e], Daniel J. Balick[f], Oskar Hallatschek[g], and Michael M. Desai[a,b,c,1]

[a]Departments of Organismic and Evolutionary Biology, [b]Physics, and [c]Faculty of Arts and Sciences Center for Systems Biology, Harvard University, Cambridge, MA 02138; [d]Department of Molecular Biology, School of Medicine, Tufts University, Boston, MA 02111; [e]Gladstone Institute of Virology and Immunology, University of California, San Francisco, CA 94158; [f]Department of Physics, University of California, Santa Barbara, CA 93106; and [g]Biophysics and Evolutionary Dynamics Group, Max Planck Institute for Dynamics and Self-Organization, 37077 Göttingen, Germany

Edited by Richard E. Lenski, Michigan State University, East Lansing, MI, and approved January 19, 2012 (received for review December 4, 2011)

When large asexual populations adapt, competition between simultaneously segregating mutations slows the rate of adaptation and restricts the set of mutations that eventually fix. This phenomenon of interference arises from competition between mutations of different strengths as well as competition between mutations that arise on different fitness backgrounds. Previous work has explored each of these effects in isolation, but the way they combine to influence the dynamics of adaptation remains largely unknown. Here, we describe a theoretical model to treat both aspects of interference in large populations. We calculate the rate of adaptation and the distribution of fixed mutational effects accumulated by the population. We focus particular attention on the case when the effects of beneficial mutations are exponentially distributed, as well as on a more general class of exponential-like distributions. In both cases, we show that the rate of adaptation and the influence of genetic background on the fixation of new mutants is equivalent to an effective model with a single selection coefficient and rescaled mutation rate, and we explicitly calculate these effective parameters. We find that the effective selection coefficient exactly coincides with the most common fixed mutational effect. This equivalence leads to an intuitive picture of the relative importance of different types of interference effects, which can shift dramatically as a function of the population size, mutation rate, and the underlying distribution of fitness effects.

Evolutionary adaptation is driven by the accumulation of beneficial mutations, and yet many aspects of this process are still poorly understood. In asexual populations, this subject can be distilled into two main lines of inquiry: (*i*) what are the possible mutations available to the population? and (*ii*) which of these mutations are actually incorporated into the population, and what are the dynamics by which they fix?

The first question is essentially an empirical matter. At any given instant in time, the set of accessible beneficial mutations is likely to depend on the history of the population as well as its environment and any epistatic interactions between mutations. Nonetheless, if history and epistatic effects do not significantly affect the statistics of the available mutations, we can define a constant distribution of fitness effects $\rho(s)$ that gives the relative probability of obtaining a mutation that increases the fitness of an individual by s.

Gillespie (1) and Orr (2) have argued that there are general theoretical reasons to expect that $\rho(s)$ should follow an exponential distribution, although more recent theoretical work has challenged the ubiquity of this claim (3). Many experimental studies are roughly consistent with this exponential prediction (4–6), although here, too, we find significant exceptions (6–10). In the present work, we maintain a relatively agnostic view toward the precise form of $\rho(s)$, although we devote special attention to the exponential case because of its popularity in the literature.

Instead, we focus our efforts on the second of the two questions listed above. Given a particular form for $\rho(s)$, what are the typical dynamics of fixation, and of all possible mutational effects, what is the distribution $\rho_f(s)$ of those that fix? Speculation about the nature of $\rho_f(s)$ dates back to the early days of population genetics, when Fisher (11) and Wright (12) fiercely debated the size of the adaptive step favored by evolution. Not only are mutations favored by $\rho_f(s)$ likely to play a prominent role in adaptation, but they are often more natural to measure experimentally than the distribution of possible mutations $\rho(s)$ (13, 14).

In small populations, or those with extremely small mutation rates, the process of adaptation is quite simple. Beneficial mutations are sufficiently rare that no more than one mutant exists in the population at any given time, and all new mutations arise on an essentially clonal background. Adaptation is therefore characterized by a series of distinct selective sweeps that occur when a new mutant rises to fixation. The probability that a new mutation fixes is simply the probability that it survives genetic drift, which is given by Haldane's formula (15) ,

$$\pi(s) \sim s. \qquad [1]$$

The distribution of fitness effects of fixed mutations immediately follows from $\rho_f(s) \propto \pi(s)\rho(s)$, which reduces the contribution from smaller mutations and leads to a slight increase in the mean effect of fixed mutations.

In larger populations the situation becomes more complicated, as many distinct mutations segregate simultaneously, but only one lineage can fix in the absence of recombination. Many of the mutations are therefore wasted, and a complicated process of interference arises between the mutations competing for fixation. This process is also found to a degree in sexual populations (the Hill–Robertson effect) if recombination cannot act quickly enough to place all of the competing mutations on the same genetic background (16).

Interference between competing mutations comes in two basic flavors. The first arises from competition between mutations with different fitness effects. A mutation **A** that has survived drift and would otherwise rise to fixation can be outcompeted by a second, stronger mutation **B** that arises before **A** has fixed. The second effect stems from competition between mutations with different genetic backgrounds. For instance, the outcompeted mutation **A** could be saved by a third mutation **C** that arises on the background of the first, such that the fitness of the double mutant **AC** exceeds that of **B** alone, allowing **A** to rise to fixation.

The first of these effects is analyzed in the theory of clonal interference (17, 18), which incorporates a distribution of fitness

Author contributions: B.H.G., I.M.R., D.J.B., O.H., and M.M.D. designed research, performed research, and wrote the paper.

The authors declare no conflict of interest.

This article is a PNAS Direct Submission.

See Commentary on page 4719.

*Previous authors occasionally use the term multiple mutants to denote those individuals that receive more than one mutation in a single generation. Here, we use the term more generally to denote lineages that receive more than one mutation before fixation. In this case, multiple mutants can be common even when multiple mutations per generation are negligible.

[1]To whom correspondence should be addressed. E-mail: mdesai@oeb.harvard.edu.

This article contains supporting information online at www.pnas.org/lookup/suppl/doi:10.1073/pnas.1119910109/-/DCSupplemental.

effects under the assumption that multiple mutants* are negligible. In this theory, new mutations are eventually fixed in the population only if they are not outcompeted by a larger mutation in the time required for them to fix, which leads to a relation between the shape of $\rho(s)$ and the rate of adaptation.

The triumph of clonal interference theory was the prediction (and subsequent experimental verification; refs. 19–21) that in large populations, the rate of adaptation increases sublinearly with the size of the population. However, it was later shown that the quantitative predictions for the rate of adaptation and the distribution of fixed mutational effects disagree with the results of simulations (22). Crucially, clonal interference theory underestimates the contribution from smaller-effect mutations, which is likely due to the neglect of multiple mutants.

Models that explicitly treat these multiple-mutation dynamics have also been analyzed in recent years (23–28) (see ref. 29 for a review), although these typically operate under the simplifying assumption that all mutations have the same effect. The primary finding of these studies is that the population forms a traveling fitness wave that moves toward higher fitness with a constant average rate v and shape $f(x)$. New mutations are eventually fixed in the population only if they occur in the best genetic backgrounds at the high-fitness nose of $f(x)$, which leads to a relation between the shape of the profile and the rate of adaptation.

By neglecting the distribution of fitness effects $\rho(s)$, multiple mutation models are able to predict the distribution of backgrounds $f(x)$. Conversely, clonal interference treats a distribution of fitness effects at the cost of neglecting the distribution of backgrounds. Of course, by explicitly ignoring the distribution of fitness effects, multiple mutation models lose any ability to make predictions about $\rho_f(s)$.

Experimental evidence suggests that both clonal interference and multiple mutations play a role in laboratory populations (30–33) (see ref. 34 for a review), their relative strengths determined by the shape of $\rho(s)$ and other population parameters. These and other results suggest that interference effects are likely to be highly relevant for many microbial and viral populations occurring in nature. Although previous theoretical work has shed light on this question through simulation studies (22, 35), infinite population models (36), and driver-mutation approximations (37), no comprehensive theory has yet emerged that accounts for both clonal interference and multiple mutation effects.

In this article, we present an analytical treatment of a distribution of fitness effects (clonal interference) as well as a distribution of backgrounds (multiple mutations) in an adapting asexual population. We leverage an approximate mathematical framework originally devised for the study of adaptation in sexual populations (38), which allows us to obtain predictions for the rate of adaptation as well as the distribution of fixed mutations in large asexual populations where mutation is weak compared to the strength of selection. We give explicit analytical solutions in the case of an exponential distribution of fitness effects, as well as a more general class of fitness distributions considered in earlier studies (22, 25, 37). We validate our results with computer simulations for a range of parameter values thought to be relevant for laboratory populations of yeast and many bacteria (30), and we show that virtually identical predictions can be obtained from exact tunable constraint models (28).

Our results confirm the intuition that the distribution of fixed mutations is strongly peaked around a single characteristic size, which depends on the underlying distribution of fitness effects as well as the population size and the mutation rate (22, 25, 39). We show that adaptation under a full distribution of fitness effects is equivalent to a second, effective theory with a single selection coefficient and rescaled mutation rate. We calculate these effective parameters, finding that the effective selection coefficient must be identified with the peak of $\rho_f(s)$. In this way, the complex interplay between clonal interference and multiple mutations works to simplify the distribution of relevant mutations. However, these relevant mutations change with $\rho(s)$, N, and U_b. This implicit dependence alters the overall scaling of the adaptation rate with population size and mutation rate, and leads to dramatic differences in the dominant mode of interference in different situations.

Analysis

We consider a population of N haploid individuals that acquire new beneficial mutations at total rate U_b. We assume that these mutations occur over a large number of loci, each with relatively small contributions to the total fitness, so that a mutation of effect s arising in an individual with (log) fitness X increases its fitness to $X + s$. Furthermore, we assume that the number of loci is sufficiently large, and epistasis sufficiently weak, that the set of available mutations can be approximated by a continuous distribution of fitness effects $\rho(s)$ that remains constant throughout the relevant time interval. We explicitly ignore transient behavior early in the adaptive process (25, 40, 41) as well as long-term changes in selection pressure as the population adapts (37, 42, 43). These remain important topics for future work. In addition, we follow previous studies (22, 24, 25) and ignore the effect of deleterious mutations, because we focus on a regime where beneficial mutations are common and deleterious mutations are expected to have a negligible effect on the dynamics of adaptation.

Our general framework is valid for a wide range of $\rho(s)$, but for the sake of concreteness we obtain explicit formulae for two specific distributions. The first of these is the exponential distribution discussed in the introduction,

$$\rho(s) = \frac{1}{\sigma} e^{-s/\sigma}, \qquad [2]$$

which has assumed the role of a null model because of its broad theoretical and experimental support. However, the ubiquity of the exponential model is by no means certain, and notable exceptions to this hypothesis have arisen in both theoretical and experimental contexts. We therefore also consider more general $\rho(s)$; as a concrete example, we describe results for a class of exponential-like distributions (22, 25, 37)

$$\rho(s) = \frac{1}{\sigma} \frac{e^{-(s/\sigma)^\beta}}{\Gamma(1+\beta^{-1})}, \qquad [3]$$

parameterized by a steepness parameter β. For large β, the sharp cutoff at $s = \sigma$ is particularly interesting because we will see that it leads to qualitatively different interference effects compared to an exponential $\rho(s)$ for similar N, U_b, and σ.

Bulk Behavior. In sufficiently large populations, it is often possible to separate the population-wide dynamics from the fate of any particular mutant (29). In this way, the distribution of fitnesses in the population can be highly predictable even though its exact genealogy is not. Previous studies have shown that large adapting populations develop into a traveling fitness wave that moves with a constant average rate v and shape $f(x)$, where $x = X - \overline{X}(t)$ measures the relative fitness of a given individual (refs. 23–28, 38, 40, 41) (Fig. 1). In principle, the shape of the wave can be rigorously determined using various methods of traveling-wave theory, such as the stochastic threshold approximation (24, 26, 40, 41), tunable constraint models (28), or stochastic fitness-class calculations (25, 27), but these methods are often difficult to apply for all but the simplest models of adaptation.

For our purposes, it will be sufficient to employ a rough approximation to the true shape of the fitness profile. Previous work has shown that in sufficiently large populations with weak mutation ($U_b \ll \sigma$, *SI Appendix*), $f(x)$ approaches a Gaussian form whose variance is equal to the rate of adaptation v (25, 40). In accordance with the earlier models (38), we therefore make the approximation that

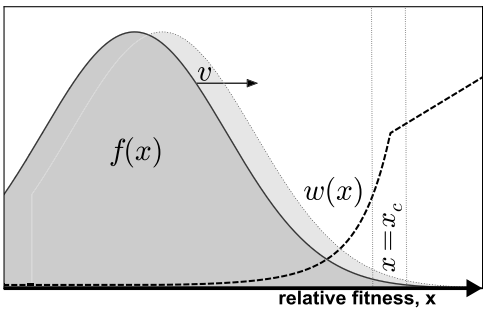

Fig. 1. A schematic illustration of the process of adaptation. The Gaussian fitness profile $f(x)$ (i.e., the distribution of backgrounds) moves at a constant rate v. The fixation probability $w(x)$ increases rapidly with x until it reaches a thin boundary layer near $x = x_c$, after which it transitions to the standard Haldane result.

$$f(x) \approx \frac{1}{\sqrt{2\pi v}} e^{-\frac{x^2}{2v}}. \quad [4]$$

Additional deviations from Eq. **4** can arise from fluctuations in the high-fitness nose of the distribution, correlated fluctuations in the mean fitness, higher mutation rates, deleterious mutations, etc., but we expect these features to play a limited role in the regimes considered here. Ultimately, this intuition can only be justified a posteriori by the generally good agreement between our analytical results and computer simulations discussed below. A more thorough discussion of the shape of the fitness profile is given in *SI Appendix*.

The Fate of Individual Lineages. From the perspective of a single lineage, competition with the rest of the population occurs only through the dynamics of the mean fitness $\overline{X}(t)$, which increases at a constant rate v in the steady state. As long as the size of the lineage remains small compared to the size of the population, we can model its behavior with a continuous-time branching process with birth rate $B(X,t) = 1 + X - \overline{X}(t)$, death rate $D = 1$, and mutation rate $U_b\rho(s)$ to fitness $X + s$.

The central quantity of interest in such models is the nonextinction probability $w(X,t)$ of a lineage founded by a single individual with fitness X at time t. Of course, any lineage that rises to fixation will eventually constitute a large fraction of the population, and our branching-process assumption starts to break down because of nonlinear effects. We assume that all lineages that avoid extinction and attain such a size are guaranteed to fix, so that we can equate $w(X,t)$ with the fixation probability of a lineage. We note that to escape the constant increase in mean fitness as the population adapts, the descendants of this individual will have to repeatedly mutate to higher fitnesses. This process is very similar to the recombinant background switching discussed by Neher et al. (38), and to the mutational surfing of genes in spatially expanding populations (44, 45).

From standard applications of branching process theory (*SI Appendix*), we can show that the fixation probability is governed by the equation

$$v\partial_x w(x) = xw(x) - w(x)^2 + U_b \int_0^\infty ds\, \rho(s)[w(x+s) - w(x)], \quad [5]$$

where we have used the fact that the fixation probability depends on X and t only through the relative fitness $x = X - \overline{X}(t)$, which satisfies $x \ll 1$ in the region of interest. For a given value of v, which is calculated self-consistently below, this equation uniquely determines the fixation probability of a new mutation for a given choice of U_b and $\rho(s)$.

Self-Consistency Condition. The individual and bulk descriptions are connected by the fact that the population ultimately adapts by producing new successful mutations. If a single mutation of effect s occurs somewhere in the population, the probability that it fixes can be obtained from $w(x)$ by averaging over the distribution of backgrounds in which it could have occurred. This average yields a generalized version of Haldane's $\pi(s)$ in the presence of interference,

$$\pi(s) = \int_{-\infty}^{\infty} dx\, w(x) f(x-s). \quad [6]$$

Consistency then requires that

$$v = \int_0^\infty ds\, s\pi(s) N U_b \rho(s). \quad [7]$$

In other words, the rate of adaptation is equal to the total rate at which new mutations fix multiplied by the size of their effect. The distribution of fixed mutations is once again obtained from the relation

$$\rho_f(s) \propto \pi(s)\rho(s). \quad [8]$$

When taken together, Eqs. **4**, **5**, and **7** fully determine the dynamics of adaptation and the distribution of fixed mutations for any combination of N, U_b, and $\rho(s)$. We examine the solutions to these equations in the following section. In *SI Appendix*, we show how this calculation can be generalized to obtain the distribution of backgrounds in which successful mutations arise, in addition to $\rho_f(s)$. We also show that nearly identical versions of Eqs. **4**, **5**, and **7** can be obtained by extending the tunable constraint framework introduced in ref. 28. This alternative formation gives a slightly more rigorous route to some of our key equations, and it suggests that the dynamics of adaptation are relatively insensitive to the particular details of our model in the large populations we consider here.

Results

Fixation Probability and the Rate of Adaptation. In the limit of large population size and weak mutation, the solution to Eq. **5** has a sharp transition at a characteristic fitness x_c, above which it will approach the linear Haldane formula for fixation in the absence of interference (Fig. 1). As shown in *SI Appendix*, we can approximate the fixation probability as

$$w(x) \approx \begin{cases} 0 & \text{if } x < 0, \\ x_c e^{\frac{x^2 - x_c^2}{2v}} & \text{if } 0 < x < x_c, \\ x & \text{if } x > x_c, \end{cases} \quad [9]$$

where x_c is determined by the condition

$$2 = U_b \int_0^\infty ds \rho(s) e^{-\frac{s^2}{2v}} \frac{e^{\frac{x_c s}{v}} - 1}{s} + U_b \int_{x_c}^\infty \frac{dx}{v} \left(\frac{x}{x_c}\right) e^{\frac{x_c^2 - x^2}{2v}} \int_0^\infty ds\, \rho(s) e^{-\frac{s^2}{2v} + \frac{xs}{v}}. \quad [10]$$

Below this transition point, Eq. **9** shows that the fixation probability is proportional to the time-integral of the deterministic lineage size, $\int n(t)dt$, which represents the total number of mutational opportunities for the lineage before it goes extinct. Intuitively then, fixation below x_c is dominated by the probability that the lineage generates a second mutant, whereas fixation above x_c is dominated by the probability that the lineage survives drift. The transition point, x_c, whereas originally arising from a purely mathematical analysis of Eq. **5**, has an intuitive interpretation as the boundary above which interference does not limit the fixation of new mutants.

We can calculate the marginal fixation probability $\pi(s)$, and hence the distribution of fixed mutations $\rho_f(s)$, by substituting our approximate form for $w(x)$ into Eq. **6** and integrating. We find

$$\pi(s) \propto e^{-\frac{s^2}{2v}}\left(\frac{e^{\frac{x_c s}{v}}-1}{s}\right)+\frac{e^{\frac{x_c^2}{2v}}}{v x_c}\int_{x_c}^{\infty} dx\, x e^{-\frac{(x-s)^2}{2v}}, \qquad [11]$$

where the normalization is determined by the condition $\pi(0) \approx 1/N$.

The fixation probability $\pi(s)$ controls the bias of those mutations that actually fix, because $\rho_f(s)$ follows immediately from $\rho_f(s) \propto \pi(s)\rho(s)$. We note here that in contrast to the original Haldane formula, $\pi(s)$ displays a regime of effective neutrality for $s < v/x_c$, where new mutations fix with a probability approximately equal to $1/N$ independent of their effect. This result agrees with the earlier findings in ref. 37. Above this threshold, the fixation probability rapidly increases before reattaining the Haldane limit for $s > x_c$. The position of these transitional points relative to the original distribution $\rho(s)$ can play a large role in the shape of the distribution of fixed mutations, as we shall see below.

The approximate expressions for $w(x)$ and $\pi(s)$ depend on the rate of adaptation v, which is self-consistently obtained by substituting Eq. **11** into the consistency condition Eq. **7**. This substitution yields a second relation between x_c and v for a given distribution $\rho(s)$. Explicit calculations for the two forms of $\rho(s)$ in Eqs. **2** and **3** are carried out in *SI Appendix*, and we summarize the main results below. In Figs. 2–4, we compare these analytical predictions to forward-time Wright–Fisher simulations.

Exponential Distribution. In the case where the distribution of fitness effects is exponential, as in Eq. **2**, we find that the integrals over the effect size s are sharply peaked around a characteristic value

$$s^* = x_c - \frac{v}{\sigma}, \qquad [12]$$

and Eqs. **10** and **7** reduce to the coupled equations

$$2 = \frac{U_b}{\sigma}\sqrt{\frac{2\pi\sigma^2}{v}}\left[1+\frac{\sigma}{x_c}+\frac{v}{\sigma x_c - v}\right]e^{\frac{(x_c-\frac{v}{\sigma})^2}{2v}}, \qquad [13]$$

$$1 = NU_b\left[\frac{x_c^2}{v}-1+\frac{2x_c\sigma}{v}+\frac{2\sigma^2}{v}\right]e^{-\frac{1}{\sigma}(x_c-\frac{v}{2\sigma})}. \qquad [14]$$

This system of transcendental equations must be solved numerically to obtain v and x_c, but we can obtain approximate analytical expressions for these quantities in two regimes of interest.

If the dominant effect size $s^* \approx x_c$, then successful mutations originating on backgrounds far from the nose of the fitness distribution are quite common. In this regime, an iterative solution

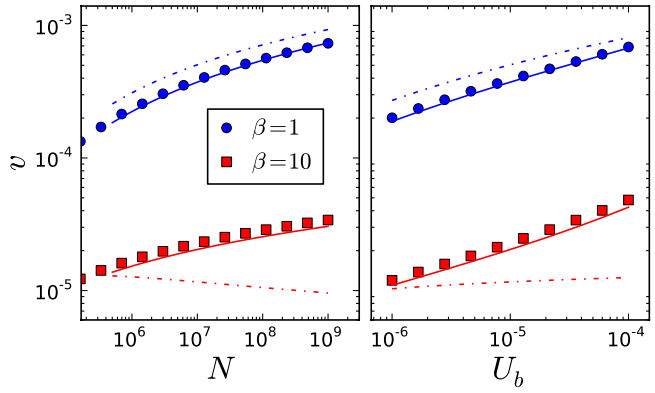

Fig. 2. The rate of adaptation, v, as a function of the population size N (*Left*) and the beneficial mutation rate U_b (*Right*) for the exponential ($\beta = 1$) and $\beta = 10$ distributions. Other parameters are $N = 10^7$, $U_b = 10^{-5}$, and $\sigma = 0.01$. Symbols denote the results of forward-time Wright–Fisher simulations, and the solid lines are obtained by solving Eqs. **13** and **14** for $\beta = 1$ and Eqs. **18** and **19** for $\beta = 10$. For comparison, the predictions from clonal interference theory are plotted as dashed lines.

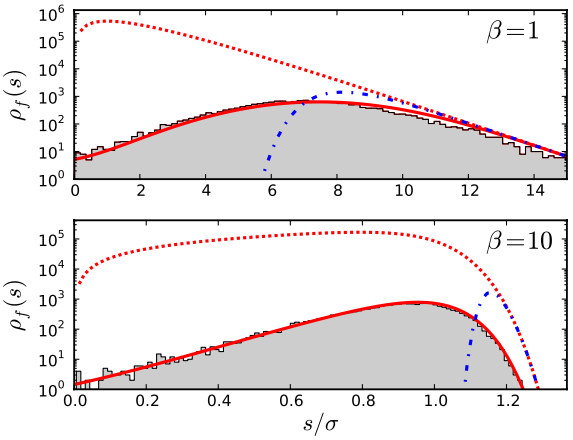

Fig. 3. The distribution of fitness effects of fixed mutations, $\rho_f(s)$, for the exponential ($\beta = 1$) (*Top*) and $\beta = 10$ (*Bottom*) distributions as measured in forward-time simulations. Other parameters are $N = 10^7$, $U_b = 10^{-5}$, and $\sigma = 0.01$. Our theoretical predictions are shown as solid red lines. For comparison, we also plot the predictions from clonal interference theory (blue dashed lines) as well as the distribution of mutational effects that would fix in the absence of interference (red dashed lines). All distributions are normalized by the total number of mutations that occur during the simulation.

of Eqs. **13** and **14** yields the approximate solution

$$v \approx \frac{\sigma^2 \log^2[2NU_b \log(\frac{\sigma}{U_b})]}{2\log\left[\frac{\sigma}{U_b}\frac{1}{\sqrt{\pi}}\frac{\log(2NU_b)}{\log^{\frac{1}{2}}(\frac{\sigma}{U_b})}\right]} \sim \frac{\sigma^2\log^2(NU_b)}{2\log(\frac{\sigma}{U_b})}, \qquad [15]$$

which self-consistently holds for the intermediate NU_b regime $\log(NU_b) \ll 2\log(\sigma/U_b)$. For extremely large NU_b, this condition will cease to be valid, and most successful mutations will originate close to the nose ($s^* \ll x_c$). In this regime, we find a different approximate expression for the adaptation rate

$$v \approx 2\sigma^2 \log[2NU_b \log(NU_b)]. \qquad [16]$$

General Distributions. More generally, the integrands in Eqs. **10** and **7** will be peaked around a characteristic s^* determined by

$$s^* - x_c - v\frac{\partial \log\rho(s^*)}{\partial s} = 0. \qquad [17]$$

If the integrals are dominated by the contribution near this peak, we can proceed in a very similar fashion to the calculation above, and we find that

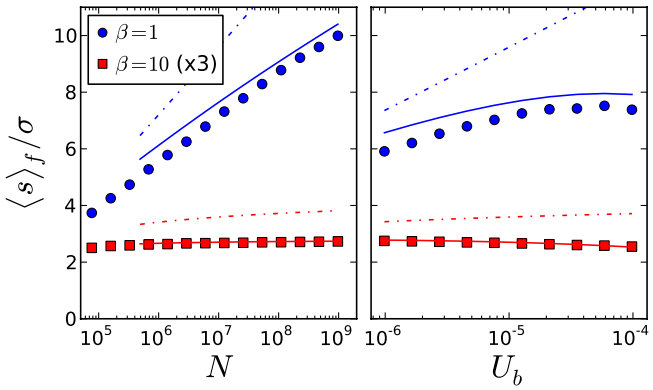

Fig. 4. The mean fitness effect of a fixed mutation as a function of the population size N (*Left*) and beneficial mutation rate U_b (*Right*) for the exponential ($\beta = 1$) and $\beta = 10$ distributions. Symbols denote the results of forward-time simulations for the parameters given in Fig. 2. Our theoretical predictions are shown as solid lines, and the predictions from clonal interference theory (dashed lines) are shown for comparison.

$$2 = \frac{U_b\sqrt{2\pi\Delta^2}\rho(s^*)}{s^*}\left[1-\frac{s^*}{x_c}\right]^{-1} e^{\frac{x_c s^*}{v}-\frac{s^{*2}}{2v}}, \quad [18]$$

$$1 = \frac{2Ns^*}{\sqrt{2\pi}}\sqrt{\frac{x_c^2}{v}}e^{-\frac{x_c^2}{2v}}, \quad [19]$$

where $\Delta = [v^{-1} - \partial_s^2 \log\rho(s^*)]^{-1/2}$ is the width of the peak. Because s^* is equivalent to the most likely fixed mutational effect (*SI Appendix*), we expect this approximation to hold whenever $\rho_f(s)$ is sufficiently peaked around a characteristic effect size. This requirement is typically satisfied for most unimodal distributions with an exponentially bounded tail (39), and in particular, for the short-tailed distributions in Eq. **3**. For $\beta \gg 1$, the characteristic effect size is

$$s^* \approx \left(\frac{x_c\sigma^\beta}{\beta v}\right)^{\frac{1}{\beta-1}}, \quad [20]$$

and the rate of adaptation is given by the approximate form

$$v \approx \frac{2\sigma^2\log[N\sigma\log^{\frac{1}{2}}(N\sigma)]}{\log^2\left[\frac{\sqrt{\beta\sigma}}{U_b}\log^{\frac{1}{2}}\left(\frac{\sqrt{\beta\sigma}}{U_b}\right)\right]}\left[1+\frac{\log(\frac{\sqrt{\beta\sigma}}{U_b})}{4\log(N\sigma)}\right]^{-2}, \quad [21]$$

which asymptotically scales as

$$v \sim \frac{2\sigma^2\log(N\sigma)}{\log^2\left(\frac{\sqrt{\beta\sigma}}{U_b}\right)}. \quad [22]$$

Note the difference in scaling compared to the exponential distribution in Eq. **15**. In this case, the scaling of v bears a much closer resemblance to earlier multiple mutation models with a single mutational effect. We explore this connection in greater detail below.

Discussion

When large populations acquire beneficial mutations, it is well-known that interference between competing lineages slows the rate of adaptation and leads to a distribution of genetic backgrounds at any given time. By explicitly accounting for this distribution of backgrounds, our analysis predicts both the rate of adaptation and the distribution of fitness effects of mutations that fix during the course of evolution, thereby offering a unified theory of interference in asexual populations.

Our analysis rests on the assumption that in large populations, the bulk dynamics of the distribution of backgrounds decouples from the fate of any particular lineage. When mutation is sufficiently weak compared to the strength of selection, we have argued that the bulk is well-approximated by a traveling fitness wave with a Gaussian profile, and the fixation probability of a given lineage depends on $U_b\rho(s)$ only through the rate of adaptation v and the transition point x_c. We observe excellent agreement between our predictions and the results of forward-time, Wright–Fisher simulations (Figs. 2–4, and our approach is further corroborated by the fact that the same mathematical structure can be deduced from an exact stochastic model of traveling waves (28) (*SI Appendix*). A virtually identical form for the fixation probability $w(x)$ arises in the study of large sexual populations (38), which suggests some sense of universality in that the dynamics of adaptation are primarily constrained by the shape and propagation of the fitness wave, rather than the exact mechanism by which lineages jump to higher fitnesses. The crucial influence of background variation on the fate of individual mutations has also been observed in laboratory populations (33), and is conjectured to hold in biparental sexual organisms as well (46).

The idea that some essential features of adaptation are insensitive to $\rho(s)$ after controlling for the speed and width of $f(x)$ is not unique. Indeed, this intuition plays a crucial role in justifying the use of multiple mutation theories to model adaptation in experimental populations (30, 39). As long as the distribution $\rho(s)$ falls off sufficiently quickly for large s, the dynamics of adaptation and the distribution of those mutations that fix will tend to be dominated by mutations of some characteristic size $\tilde{s}$. Those mutations with $s < \tilde{s}$ will typically be outcompeted by mutations of larger effect, whereas mutations with $s > \tilde{s}$ are too rare to occur before a fitter multiple mutant establishes. Thus, the dynamics of adaptation can be equivalently described by a multiple mutations model with a single, effective selection coefficient and mutation rate despite a full underlying distribution $\rho(s)$.

Our results confirm this general intuition [although in some cases the dispersion in $\rho_f(s)$ can be rather large, Fig. 3*A*], and our analytical description allows us to make this statement quantitatively precise. Carrying out the calculations above for the single-s distribution $U_b\rho(s) = U_{\text{eff}}\delta(s - s_{\text{eff}})$ (*SI Appendix*), we look for effective parameters s_{eff} and U_{eff} such that our approximate solutions for v and $w(x)$ match those for the original distribution. As long as $\rho_f(s)$ is strongly peaked around a typical effect size, Eqs. **18** and **19** imply that this single-s equivalence holds if and only if

$$s_{\text{eff}} = s^*, \qquad U_{\text{eff}} = U_b\sqrt{2\pi\Delta^2}\rho(s^*), \quad [23]$$

where s^* and Δ are given above. In other words, the effective selection coefficient exactly coincides with the most probable fixed effect, and the effective mutation rate is scaled by the probability of observing that mutation under the original distribution $\rho(s)$. By construction, the predictions of our theory for this single-s model with effective parameters s_{eff} and U_{eff} exactly match the predictions of our theory for the full $\rho(s)$. We note, however, that because the effective parameters themselves depend on N, U_b, and $\rho(s)$, the dependence of v on population size and mutation rate will differ from a true single-s theory, which could be used to distinguish the underlying distribution of fitness effects experimentally.

Although the mapping defined by Eq. **23** is always valid, it can be instructive to consider an even simpler single-s mapping in the special case that $x_c \approx s^*$, which occurs for the exponential distribution in the intermediate-NU_b regime. In this case, a more intuitive understanding of the dynamics can be obtained by mapping to a selective sweeps model where the rate of adaptation is given by the well-known formula $v = NU_{\text{eff}}s_{\text{eff}}^2$. We again find that s_{eff} and U_{eff} are given by Eq. **23** if we define an effective population size

$$N_{\text{eff}} = N\left(\frac{v}{x_c - s^*}\right)f\left(\frac{x_c - s^*}{v}\right), \quad [24]$$

which accounts for the fact that mutations typically arise from a background with fitness $x \approx x_c - s^*$ rather than from the wild-type fitness (*SI Appendix*).

These different effective models reflect dramatic differences in the typical dynamics of fixation. For the large-NU_b exponential regime and the $\beta \gg 1$ distributions, successful mutations typically arise on backgrounds at the nose of the wave and mutate to fitnesses near the interference threshold x_c. Multiple mutations of size s^* are therefore essential for fixation, and the background in which each mutant arises plays a central role in its ultimate chance of fixation. On the other hand, for the intermediate-NU_b exponential regime, typical mutations arise from the bulk of the fitness profile and mutate to fitnesses near x_c. Thus, the background on which they arise is less important; fixations are dominated by a single driving mutation which can leapfrog all other variation in the population. However, this behavior differs from the standard selective sweeps or clonal interference picture in that new driving mutations typically arise before the previous mutation has fixed.

Recent work by Schiffels et al. (37) has leveraged this driving mutation approximation to study adaptation under an exponen-

tial $\rho(s)$, similar to the case considered here. By adding passenger-mutation corrections, they also correctly predict the rate of adaptation and the distribution of fixed mutations observed in Fig. 3*A*, thereby offering further evidence for our interpretation above. This work provides an accurate and interesting complement to our analysis in the intermediate-NU_b regime where single driving mutations dominate the dynamics. However, our results show that this approximation breaks down for larger NU_b, and also does not hold for more general distributions (e.g., $\beta \gg 1$) when $\rho(s)$ decreases much faster than exponentially. In these cases, we obtain a qualitatively different picture of interference in which multiple driving mutations play a dominant role. By successfully accounting for both extremes, the present framework (and the corresponding single-s mappings) can help predict the degree to which we might expect more clonal interference or multiple mutation effects for a given set of parameters.

This discussion also suggests possible experimental tests of our theory using experimental evolution. For a given distribution of fitness effects $U_b\rho(s)$, our framework provides concrete predictions for the most accessible experimental quantities: the rate of adaptation and the distribution of fixed mutational effects. By measuring how these quantities vary with N, we can directly probe our theoretical predictions. Combining these results with measurements of the fitness variation maintained by a population (30) and with direct genomic information from adapted lineages to measure the distribution of backgrounds on which successful mutations arise (47), we can further test our predicted picture of the typical mode of adaptation, and observe how this mode changes as a function of population size.

Up to this point, we have focused exclusively on beneficial mutations. This focus was justified on the basis of earlier studies (22, 24, 25) that find that deleterious mutations have a negligible effect on the dynamics of adaptation when beneficial mutations are common. Nevertheless, because the vast majority of available mutations in real populations are likely to be neutral or deleterious, it would be desirable to extend our theory to explicitly account for these mutations. If we can safely ignore the effects of deleterious mutations on the dynamics of adaptation, their fixation probabilities follow the form of $\pi(s)$ calculated above, which rapidly decays for $s < 0$. However, as the ratio of deleterious to beneficial mutations increases, we eventually expect these mutations to alter the dynamics of adaptation itself, which will in turn effect the distribution of fixed mutations. We aim to explore this dependence in detail in a future paper.

ACKNOWLEDGMENTS. We thank John M. Coffin, Richard A. Neher, and Boris I. Shraiman for comments and useful discussions. This work was supported in part by a National Science Foundation Graduate Research Fellowship (B.H.G.), the Max Planck Society (O.H.), and the James S. Mcdonnell Foundation and the Harvard Milton Fund (M.M.D). I.M.R. was supported by National Institute of Health Grants R01AI 063926 (to I.M.R.) and R37CA 089441 (to John M. Coffin). D.J.B. was supported by National Institutes of Health Grant R01GM 086793 (to Boris I. Shraiman). Simulations in this paper were performed on the Odyssey cluster supported by the Research Computing Group at Harvard University.

1. Gillespie J (1984) Molecular evolution over the mutational landscape. *Evolution* 38:1116–1129.
2. Orr H (2003) The distribution of fitness effects among beneficial mutations. *Genetics* 163:1519–1526.
3. Joyce P, Rokyta D, Beisel C, Orr H (2008) A general extreme value theory model for the adaptation of DNA sequences under strong selection and weak mutation. *Genetics* 180:1627–1643.
4. Imhof M, Schlötterer C (2001) Fitness effects of advantageous mutations in evolving *Escherichia coli* populations. *Proc Natl Acad Sci USA* 98:1113–1117.
5. Kassen R, Bataillon T (2006) Distribution of fitness effects among beneficial mutations before selection in experimental populations of bacteria. *Nat Genet* 38:484–488.
6. MacLean R, Buckling A (2009) The distribution of fitness effects of beneficial mutations in *Pseudomonas aeruginosa*. *PLoS Genet* 5 e1000406.
7. Sanjuán R, Moya A, Elena SF (2004) The distribution of fitness effects caused by single-nucleotide substitutions in an RNA virus. *Proc Natl Acad Sci USA* 101:8396–8401.
8. Cowperthwaite MC, Bull J, Meyers LA (2005) Distributions of beneficial fitness effects in RNA. *Genetics* 170:1449–1457.
9. Barrett RD, MacLean RC, Bell G (2006) Mutations of intermediate effect are responsible for adaptation in evolving *Pseudomonas fluorescens* populations. *Biol Lett* 2:236–238.
10. Rokyta DR, et al. (2008) Beneficial fitness effects are not exponential for two viruses. *J Mol Evol* 67:368–376.
11. Fisher RA (1930) *The Genetical Theory of Natural Selection* (Oxford Univ Press, Oxford), Chap 4.
12. Wright S (1931) Evolution in mendelian populations. *Genetics* 16:97–159.
13. Rozen DE, de Visser JA, Gerrish PJ (2002) Fitness effects of beneficial mutations in microbial populations. *Curr Biol* 12:1040–1045.
14. Parfeito L, Fernandes L, Mota C, Gordo I (2007) Adaptive mutations in bacteria: High rate and small effects. *Science* 317:813.
15. Haldane J (1927) The mathematical theory of natural and artificial selection, part v: Selection and mutation. *Proc Cambridge Philos Soc* 23:828–844.
16. Hill WG, Robertson A (1966) Effect of linkage on limits to artificial selection. *Genet Res* 8:269–294.
17. Gerrish P, Lenski R (1998) The fate of competing beneficial mutations in an asexual population. *Genetica* 102–103:127–144.
18. Wilke CO (2004) The speed of adaptation in large asexual populations. *Genetics* 167:2045–2053.
19. Miralles R, Gerrish PJ, Moya A, Elena SF (1999) Clonal interference and the evolution of RNA viruses. *Science* 285:1745–1747.
20. de Visser JAGM, Zeyl CW, Gerrish PJ, Blanchard JL, Lenski RE (1999) Diminishing returns from mutation supply rate in asexual populations. *Science* 283:404–406.
21. Colegrave N (2002) Sex releases the speed limit on evolution. *Nature* 420:664–666.
22. Fogle CA, Nagle JL, Desai MM (2008) Clonal interference, multiple mutations and adaptation in large asexual populations. *Genetics* 180:2163–2173.
23. Tsimring L, Levine H, Kessler D (1996) RNA virus evolution via a fitness-space model. *Phys Rev Lett* 90:088103.
24. Rouzine IM, Wakeley J, Coffin JM (2003) The solitary wave of asexual evolution. *Proc Natl Acad Sci USA* 100:587–592.
25. Desai MM, Fisher DS (2007) Beneficial mutation selection balance and the effect of genetic linkage on positive selection. *Genetics* 176:1759–1798.
26. Rouzine I, Brunet E, Wilke C (2008) The traveling-wave approach to asexual evolution: Muller's ratchet and the speed of adaptation. *Theor Pop Biol* 73:24–46.
27. Brunet E, Rouzine IM, Wilke CO (2008) The stochastic edge in adaptive evolution. *Genetics* 179:603–620.
28. Hallatschek O (2011) The noisy edge of traveling waves. *Proc Natl Acad Sci USA* 108:1783–1787.
29. Park S, Simon D, Krug J (2010) The speed of evolution in large asexual populations. *J Stat Phys* 138:381–410.
30. Desai MM, Fisher DS, Murray AW (2007) The speed of evolution and the maintenance of variation in asexual populations. *Curr Biol* 17:385–394.
31. Pepin KM, Wichman HA (2008) Experimental evolution and genome sequencing reveal variation in levels of clonal interference in large populations of bacteriopage ϕx174. *BMC Evol Biol* 8:85–98.
32. Miller CR, Joyce P, Wichman HA (2011) Mutational effects and population dynamics during viral adaptation challenge current models. *Genetics* 187:185–202.
33. Lang GI, Botstein D, Desai MM (2011) Genetic variation and the fate of beneficial mutations in asexual populations. *Genetics* 188:647–661.
34. Sniegowski PD, Gerrish PJ (2010) Beneficial mutations and the dynamics of adaptation in asexual populations. *Philos Trans R Soc B* 365:1255–1263.
35. Kim Y, Orr H (2005) Adaptation in sexuals vs. asexuals: Clonal interference and the Fisher–Muller model. *Genetics* 171:1377–1386.
36. Park S, Krug J (2007) Clonal interference in large populations. *Proc Natl Acad Sci USA* 104:18135–18140.
37. Schiffels S, Szöllösi G, Mustonen V, Lässig M (2011) Emergent neutrality in adaptive asexual evolution. *Genetics* 189:1361–1375.
38. Neher R, Shraiman BI, Fisher DS (2010) Rate of adaptation in large sexual populations. *Genetics* 184:467–481.
39. Hegreness M, Shoresh N, Hartl D, Kishony R (2006) An equivalence principle for the incorporation of favorable mutations in asexual populations. *Science* 311:1615–1617.
40. Rouzine IM, Coffin JM (2005) Evolution of HIV under selection and weak recombination. *Genetics* 170:7–18.
41. Rouzine IM, Coffin JM (2010) Many-site adaptation in the presence of infrequent recombination. *Theor Pop Biol* 77:189–204.
42. Mustonen V, Lässig M (2008) Molecular evolution under fitness fluctuations. *Phys Rev Lett* 100:108101.
43. Mustonen V, Lässig M (2009) From fitness landscapes to seascapes: Non-equilibrium dynamics of selection and adaptation. *Trends Genet* 25:111–119.
44. Hallatschek O, Nelson DR (2008) Gene surfing in expanding populations. *Theor Popul Biol* 73:158–170.
45. Excoffier L, Ray N (2008) Surfing during population expansions promotes genetic revolutions and structuration. *Trends Ecol Evol* 23:347–351.
46. Barton NH, Etheridge AM (2011) The relation between reproductive value and genetic contribution. *Genetics* 188:953–973.
47. Barrick JE, et al. (2009) Genome evolution and adaptation in a long-term experiment with *Escherichia coli*. *Nature* 461:1243–1247.

The Rate of Adaptation and the Distribution of Fixed Beneficial Mutations in Asexual Populations: Supplementary Information

Benjamin H. Good,[1] Igor M. Rouzine,[2,3] Daniel J. Balick,[4] Oskar Hallatschek,[5] and Michael M. Desai[1]

[1] *Departments of Organismic and Evolutionary Biology and of Physics and FAS Center for Systems Biology, Harvard University, Cambridge, MA*
[2] *Department of Molecular Biology, School of Medicine, Tufts University, Boston, MA*
[3] *Gladstone Institute of Virology and Immunology, San Francisco, CA*
[4] *Department of Physics, University of California, Santa Barbara, CA*
[5] *Biophysics and Evolutionary Dynamics Group, Max Planck Institute for Dynamics and Self-Organization, Göttingen, Germany*

APPENDIX A: THE DISTRIBUTION OF BACKGROUNDS

Our analysis in the main text is simplified by our assumption that the distribution of backgrounds, $f(x)$, can be approximated by the Gaussian form

$$f(x) \approx \frac{1}{\sqrt{2\pi v}} e^{-\frac{x^2}{2v}}, \tag{A1}$$

where v is the average rate of adaptation. This approximation has arisen several times in earlier (single-s) treatments of adaptation [1–4] and is based on simple deterministic growth under the action of selection alone. For the purposes of our paper — which incorporates $f(x)$ into a theory of interference in adapting asexual populations — this crude approximation suffices because it leads to highly accurate predictions for v and ρ_f, and it illustrates the main point in a simple manner.

Nevertheless, a more rigorous derivation of $f(x)$ from first principles would be greatly desirable, both for the sake of completeness as well as for those regimes where Eq. (A1) starts to break down. A full derivation is beyond the scope of the present work, but we outline the main idea below.

Let $n(X,t)$ denote the number of individuals with absolute fitness X at time t. These fitness classes evolve according to the stochastic integro-differential equation

$$\frac{\partial n(X,t)}{\partial t} = \left[X - \overline{X}(t)\right] n(X,t) + U_b \int_0^\infty ds\, \rho(s) \left[n(X-s,t) - n(X,t)\right] + \sqrt{2n(X,t)}\eta(X,t), \tag{A2}$$

where $\overline{X}(t) = \frac{1}{N}\int dX\, X n(X,t)$ is the mean fitness of the population and $\eta(X,t)$ denotes a complicated noise term arising from the stochastic dynamics of reproduction and the finite population constraint. For any particular population, the full profile of $n(X,t)$ consists of a relatively small set of δ-functions where particular lineages have established. It is only by averaging over many possible instances and their corresponding fluctuations that we can obtain the continuous version in Eq. (A1). Traveling wave theory [2, 3, 5, 6] and tunable constraint models (see Appendix C) give two different prescriptions for obtaining the mean-field profile $f(X,t)$, which is roughly defined as

$$f(X,t) \approx \left\langle \frac{n(X,t)}{N} \right\rangle. \tag{A3}$$

Both predict a stochastic threshold at some characteristic relative fitness $x_{\rm edge}$, above which the fitness profile rapidly decays to zero. Below this threshold, the effect of the noise term $\eta(X,t)$ on the mean profile $f(X,t)$ can be neglected. In order to obtain a fully deterministic description of $f(X,t)$, we must make the additional assumption that the stochastic mean fitness $\overline{X}(t)$ can be replaced by its average value

$$\overline{X}(t) \approx \left\langle \overline{X}(t) \right\rangle = vt + \text{constant}. \tag{A4}$$

This assumption can be violated in the steady-state due to correlated fluctuations in the rate of adaptation and the shape of the wave, but we assume that these fluctuations have a negligible impact on the large-scale dynamics of adaptation.[1] After switching to the co-moving frame and rewriting everything in terms of the relative fitness

[1] Even in cases where these fluctuations are negligible on a macroscopic scale, we must be careful about equating the "theoretical" relative fitness $x = X - vt$ with the the *actual* relative fitness $X - \overline{X}(t)$ as measured in simulations or experiments. This is especially true for small x, when the typical fluctuations in $\overline{X}(t)$ are comparable to x. As a result, *direct* comparisons of $f(X,t)$ with the observed shape will have limited utility when the typical fluctuations are on the order of the standard deviation of the wave profile.

$x = X - vt$, the shape of the wave below the stochastic threshold is described by the deterministic differential equation

$$-v\partial_x f(x) = xf(x) + U_b \int_0^\infty ds\, \rho(s)\left[f(x-s) - f(x)\right] . \tag{A5}$$

The Gaussian profile in Eq. (A1) is just the solution to this equation when $U_b = 0$. It is also the leading order solution for $U_b > 0$ if the mutational term is small, or

$$xe^{-\frac{x^2}{2v}} \gg U_b \int_0^\infty ds\, \rho(s)\left[e^{-\frac{(x-s)^2}{2v}} - e^{-\frac{x^2}{2v}}\right] , \tag{A6}$$

for the relevant regions of x. In the case where $\rho(s)$ is exponential, we can verify that this condition holds near the most likely background fitness $x = x_c - s^*$ as long as

$$\frac{x_c - s^*}{\sqrt{v}} \frac{\sigma}{U_b} \gg 1 , \tag{A7}$$

which is certainly satisfied for the parameter regimes considered here. For the more general class of distributions analyzed in Appendix F, we can leverage our approximate analytical calculations to show that a sufficient condition for Eq. (A6) to hold near $x = x_c - s^*$ is

$$x_c \gg s^* , \tag{A8}$$

in addition to the other assumptions required by Appendix D and Appendix F. This will be true for the $\beta = 10$ distribution in the parameter ranges considered here.

In general, however, the fitness profile must be derived by solving Eq. (A5) (or its counterpart in Eq. (C6)), and substituting it into the consistency condition for the velocity in Eqs. (6) and (7) in the main text. In particular, we expect the simple Gaussian approximation to break down for large mutation rates, where the mutational term leads to nontrivial modifications of the wave shape [7].

In addition, we note that the Gaussian approximation appears to yield good quantitative results, even though we continue this approximation well beyond the stochastic cutoff found in traveling wave theory or tunable constraint models (see Appendix C). This stands in contrast to earlier single-s theories, which emphasize that the dynamics are also strongly influenced by the shape of $f(x)$ near the high-fitness nose of the distribution [1, 2, 7–9]. In the present work, we find that the dominant contributions to integrals over $f(x)$ always occur for $x < x_c$, so the exact behavior above the cutoff may be unimportant in this case. A more thorough analysis of this aspect of the theory and the ways in which x_c relates to the stochastic cutoff in earlier models will be explored in future work.

APPENDIX B: DERIVATION OF THE MASTER EQUATION

Given a model of the bulk behavior of the population, our second key assumption is that after conditioning on this bulk behavior, individual lineages go extinct or fix independently. This allows us to consider the fixation probability of a single lineage in isolation, without having to worry about the *joint* fixation probabilities of all extant lineages in the population.

We take advantage of the fact that in large populations, the exact stochastic dynamics of reproduction have a negligible impact on macroscopic quantities like v and $\rho_f(s)$ [1, 5]. At most, different models of reproduction lead to an $O(1)$ constant multiplying N in the various formulae that follow. This allows us to choose the simplest stochastic model available without worrying whether the microscopic details match those in natural organisms. In our case, this means that we choose to model the dynamics of individual lineages using a continuous-time branching process with birth rate $B(X,t) = 1 + X - \overline{X}(t)$, death rate $D = 1$, and mutations to fitness $X + s$ at rate $U_b\rho(s)$. We derive a master equation for the fixation probability of a single individual below.

Let $p(n, X, t)$ be the extinction probability of a lineage with n individuals at time t with absolute fitness X. By explicitly considering birth, death, and mutation events, we obtain the backward master equation

$$\begin{aligned} p(n, X, t-dt) = {} & \underbrace{\left[1 - ndt(2 + X - \overline{X}(t) + U_b)\right]}_{\text{Prob[nothing happened]}} p(n, X, t) + \underbrace{ndt(1 + X - \overline{X}(t))}_{\text{Prob[birth]}} p(n+1, X, t) \\ & + \underbrace{ndt}_{\text{Prob[death]}} p(n-1, X, t) + \underbrace{ndtU_b \int_0^\infty ds\, \rho(s)}_{\text{Prob[mutation event]}} p(1, X+s, t)p(n-1, X, t) . \end{aligned} \tag{B1}$$

Taking the continuous-time limit, we can rewrite this as

$$-\frac{1}{n}\partial_t p(n,X,t) = -[2+X-\overline{X}(t)+U_b]p(n,X,t) + [1+X-\overline{X}(t)]p(n+1,X,t) + p(n-1,X,t) + U_b\int_0^\infty ds\,\rho(s)p(1,X+s,t)p(n-1,X,t)\,. \tag{B2}$$

By assumption, each lineage goes extinct independently, which implies that

$$p(n,X,t) = p(1,X,t)^n\,, \tag{B3}$$

and hence

$$-\partial_t p(1,X,t) = -[2+X-\overline{X}(t)+U_b]p(1,X,t) + [1+X-\overline{X}(t)]p(1,X,t)^2 + 1 + U_b\int_0^\infty ds\,\rho(s)p(1,X+s,t)\,. \tag{B4}$$

The fixation probability of an individual, $w(X,t)$, is related to the extinction probability through the relation

$$w(X,t) = 1 - p(1,X,t)\,, \tag{B5}$$

so we can simply substitute into Eq. (B4) to obtain

$$-\partial_t w(X,t) = [X-\overline{X}(t)-U_b]w(X,t) - [1+X-\overline{X}(t)]w(X,t)^2 + U_b\int_0^\infty ds\,\rho(s)w(X+s,t)\,. \tag{B6}$$

Due to time-translation symmetry, it is clear that the fixation probability of an individual can depend on the absolute fitness and the absolute time only through the relative fitness

$$x = X - \overline{X}(t)\,. \tag{B7}$$

This allows us to replace time derivatives with spatial derivatives, $\partial_t \to -v\partial_x$, and yields an ordinary differential equation for $w(x)$:

$$v\partial_x w(x) = xw(x) - (1+x)w(x)^2 + U_b\int_0^\infty ds\,\rho(s)\left[w(x+s)-w(x)\right]\,. \tag{B8}$$

We obtain Eq.(5) in the main text by making the additional assumption that selection acts over time-scales much longer than a single generation, which implies that $x \ll 1$. This is simply an alternate way to state that all relevant selection pressures are small.

APPENDIX C: RELATIONSHIP TO TUNABLE CONSTRAINT MODELS

The results in the main text were presented in the context of the "deterministic profile/independent fixation" approach outlined above, but it is interesting to note that we can also formulate our theory in terms of the tunable constraint framework introduced in [9]. The advantage of this alternate formulation is that we can write down an *exact* set of differential equations for the average fitness profile $f(x)$ and the fixation probability $w(x)$ that naturally account for the stochastic nature of the high-fitness "nose" and correlated fluctuations in the mean fitness. Unfortunately, this considerable simplification is gained by treating a different model of the stochastic dynamics (see below), and there is no guarantee that the predictions of these "exactly solvable models" will show better agreement with Wright-Fisher simulations. Nevertheless, we find that in the regimes considered here, the tunable constraint predictions are identical with those presented in the main text (up to a replacement $N \to N/2$ in our expressions for v and $\rho_f(s)$ arising from the different stochastic dynamics).

In the tunable constraint model, the population evolves in time according to a two-step process for each infinitesimal time interval dt. First, the fitness class sizes $n(X,t)$ evolve according to

$$\frac{\partial n(X,t)}{\partial t} = [X-vt]\,n(X,t) + U_b\int_0^\infty ds\,\rho(s)\left[n(X-s,t)-n(X,t)\right] + \sqrt{2n(X,t)}\eta(X,t)\,, \tag{C1}$$

which differs from Eq. (A2) in that the nonlinear selection term has been replaced with the linear version

$$\left[X - \frac{\int dX\,Xn(X,t)}{\int dX\,n(X,t)}\right]n(X,t) \to [X-vt]\,n(X,t)\,, \tag{C2}$$

and $\sqrt{2n(X,t)}\eta(X,t)$ corresponds to the noise term in an *unconstrained* birth-death process, with

$$\langle \eta(X,t)\rangle = 0\,, \quad \langle \eta(X,t)\eta(X',t)\rangle = \delta(X-X')dt\,. \tag{C3}$$

In the second step, the population is uniformly culled to enforce the constraint

$$\int dx\, n(x+vt,t)\tilde{w}(x) = 2\,, \tag{C4}$$

where $\tilde{w}(x)$ is some arbitrary deterministic *constraint function* that is constant in time. When $\tilde{w}(x)$ is independent of x, we recover the normal "fixed-N" constraint of the Wright-Fisher model, but in general Eq. (C4) allows for fluctuations in the population size.

Taken together, Eqs. (C1) and (C4) completely determine the stochastic dynamics in the tunable constraint model, and we define the wave shape $f(x)$ to *exactly* coincide with the average

$$f(x) = \left\langle \frac{n(x+vt,t)}{N} \right\rangle . \tag{C5}$$

Following the derivation in [9], it can be shown that if we choose $\tilde{w}(x)$ to coincide with the non-extinction probability $w(x)$ defined the main text, then $f(x)$ and $w(x)$ jointly satisfy the closed system of equations

$$-v\partial_x f(x) = xf(x) + U_b \int_0^\infty ds\, \rho(s)\left[f(x-s) - f(x)\right] - w(x)f(x)\,, \tag{C6}$$

$$v\partial_x w(x) = xw(x) + U_b \int_0^\infty ds\, \rho(s)\left[w(x+s) - w(x)\right] - w(x)^2\,, \tag{C7}$$

and

$$\int f(x)w(x) = \frac{2}{N}\,. \tag{C8}$$

[The notation in [9] involved two functions $u^*(x)$ and $\bar{c}(x)$ for the fixation probability and mean number density, respectively. In terms of the notation of the present paper, these functions are given by $u(x)^* \equiv w(x)/2$ and $\bar{c}(x) \equiv Nf(x)$.]

Note that Eq. (C6) is identical to the deterministic equation for the fitness profile in Appendix A up to the addition of the nonlinear term $w(x)f(x)$, which enforces the stochastic cutoff at the nose. This term is negligible when $w(x) \ll x$ or when $x < x_c$, so long as our usual "sharpness" condition $x_c \gg \sqrt{v}$ is satisfied. Similarly, Eq. (C7) is just the defining equation for the non-extinction probability that we employ in the main text. It was shown in [9] that $w(x)/2$ can be identified with the fixation probability of an individual at relative fitness x in this model, so the consistency condition in Eq. (C8) is equivalent to the statement that the entire population must eventually descend from a single individual.

Together, Eqs. (C6), (C7), and (C8) fully determine the rate of adaptation and the distribution of fixed mutational effects as a function of N, U_b, and $\rho(s)$. In the tunable constraint framework it is most natural to use the consistency condition in Eq. (C8) because it is directly related to the finite population constraint that was used to introduce $\tilde{w}(x)$. However, we can also show that Eqs. (C6), (C7), and (C8) automatically imply that the consistency condition in Eq. [7] in the main text is satisfied as well. To see this, we begin by multiplying both sides of Eq. (C6) by $xw(x)$ and integrating over x. The term on the left-hand side becomes

$$\int_{-\infty}^\infty dx\, xw(x)\left[-v\partial_x f(x)\right] = v\left(\frac{N}{2}\right) + \int_{-\infty}^\infty dx\, xfv\partial_x w\,, \tag{C9}$$

where we have used the consistency condition Eq. (C8). After making the change of variables $x - s \to x$, the second term on the right can be written in the form

$$\int_{-\infty}^\infty dx\, xw(x)U_b \int_0^\infty ds\, \rho(s)f(x-s) = \int_0^\infty ds \int_{-\infty}^\infty dx\, (x+s)w(x+s)U_b\rho(s)f(x) \tag{C10}$$

$$= \int_{-\infty}^\infty xf(x)U_b \int_0^\infty ds\, \rho(s)w(x+s) + \int_0^\infty ds\, s\rho(s)U_b \int_{-\infty}^\infty dx\, f(x-s)w(x)\,. \tag{C11}$$

Putting everything together, we see that

$$v\left(\frac{N}{2}\right)+\int_{-\infty}^{\infty}dx x f\, v\partial_x w = \int_0^\infty ds\, s\rho(s)U_b\int_{-\infty}^{\infty}dx\, f(x-s)w(x) + \int_{-\infty}^{\infty}xf(x)\left\{xw(x)+U_b\int_0^\infty ds\,\rho(s)\left[w(x+s)-w(x)\right]-w(x)^2\right\}, \tag{C12}$$

or

$$v=\int_0^\infty ds\, s\rho(s)\left(\frac{N}{2}\right)U_b\int_{-\infty}^{\infty}dx\, f(x-s)w(x)\,, \tag{C13}$$

where we have used the equations of motion for $w(x)$ in Eq. (C7).

Thus, we see that up to the nonlinear cutoff in Eq. (C6), this tunable constraint model is equivalent to the considerably more ad-hoc approach outlined in the main text. It is interesting to see that many of our assumptions in the original framework can be derived more rigorously from the tunable constraint perspective whenever the nonlinear cutoff in Eq. (C6) can be neglected.

However, this increased rigor does not necessarily imply increased correctness when comparing to fixed-N simulations, since it describes the solution to a different stochastic process. The population size fluctuates in the tunable constraint model, while the relative growth rate x (and therefore the location of the edge) is defined in a deterministic manner. In Wright-Fisher simulations, the population size is fixed while relative growth rate is given by the random variable $X-\overline{X}(t)$.

Yet we find that in the regimes where at least one of our models is relevant, they are both valid descriptions of the dynamics (though there may be slight quantitative disagreements due to the aforementioned $N\to N/2$ replacement). This agreement between fixed-N models and their tuned counterparts has been observed earlier [9], and it indicates that the dynamics of adaptation are quite robust to population size fluctuations. In fact, since most quantities of interest depend only logarithmically on N, one may speculate that population size fluctuations do not strongly affect the dynamics as long as fluctuations in $\log N$ are small. This insensitivity to fluctuations in N gives some hope that these simple models may also be applicable to real (well-mixed) systems with unknown demographic history.

APPENDIX D: ANALYSIS OF THE FIXATION PROBABILITY

In Appendix B and Appendix C , we argued that the fixation probability of a single individual with relative fitness x satisfies the integro-differential equation

$$\underbrace{v\partial_x w(x)}_{V}=\underbrace{xw(x)}_{S}+\underbrace{U_b\int_0^\infty ds\,\rho(s)\left[w(x+s)-w(x)\right]}_{M}-\underbrace{w(x)^2}_{N}, \tag{D1}$$

where we have now explicitly labeled the velocity (V), selection (S), mutation (M), and nonlinear (N) terms. This equation comes with the implicit boundary condition that $w(x)$ is finite for all x, which should remove the constant of integration associated with the derivative in the velocity term. Of course, an exact analytical solution to this equation for arbitrary $\rho(s)$ would completely solve our problem, but the difficulty involved in solving any integro-differential equation suggests that an exact solution is presently beyond our reach.

We do notice, however, that the integral is entirely contained in the M term, which suggests that we may be able to develop a perturbative solution to this problem in the limit that M is in some sense small. This plan is complicated by the fact that our perturbative theory will actually be *singular* in the limit that $M\to 0$, because the mutation term plays a crucial role in regulating the behavior of the solution. If $M=0$, the only solution that does not diverge for finite x is the trivial solution $w(x)=0$, which agrees with our intuition that a lineage cannot survive the constant increase of $\overline{X}(t)$ without the ability to mutate to higher fitnesses. Thus, the leading-order solution as $M\to 0$ is *not* the same as the solution to Eq. (D1) with $M=0$.

Nevertheless, it will still be the case that M can be negligible in certain *regions* even though it cannot be negligible on a global scale. The local analysis that follows is essentially the same as the one in Neher *et al* [4], which focused on a regime where recombination is the dominant mechanism for increasing fitness. We show how this framework can be extended to the case of mutation-dominated adaptation below.

For large positive x, a typical lineage will either die or be destined for fixation long before additional mutations or the steady increase of the mean fitness can significantly affect its growth rate. Thus, in this region, the dominant balance in Eq. (D1) is given by the S and N terms, which yields the approximate solution

$$w(x)\approx x\,. \tag{D2}$$

Note that this is simply the ordinary Haldane formula for the fixation probability of a single individual with fitness x [10]. This balance is consistent as long as the V and M terms are small, which occurs when

$$x^2 \gg v\,, \tag{D3}$$

$$x^2 \gg U_b \int_0^\infty ds\, \rho(s) s\,. \tag{D4}$$

As we look towards smaller x, we will eventually reach a point where the steady increase in $\overline{X}(t)$ can have a significant impact on the eventual fixation of a lineage. In this "interference" regime, the fixation probability of a lineage is greatly reduced, and the nonlinear term becomes negligible. If the mutation term can also be treated as small, the dominant balance in this regime is given by the V and S terms, which yields the approximate solution

$$w(x) \approx A e^{\frac{x^2}{2v}}\,, \tag{D5}$$

where A is a constant of integration. If $x = x_c$ denotes the location of the boundary between the interference and drift regimes, this constant can be determined by matching the two solutions at $x = x_c$. This yields

$$A = x_c e^{-\frac{x_c^2}{2v}}\,. \tag{D6}$$

After substituting this solution back into Eq. (D1), we can verify that the nonlinear term is negligible as long as

$$\left(\frac{x_c}{x}\right) e^{\frac{x^2 - x_c^2}{2v}} \ll 1\,, \tag{D7}$$

which will be true for x close to x_c as long as $x_c \gg \sqrt{v}$. The rate at which the nonlinear term decreases for $x < x_c$ can be used to define an effective width of the boundary layer between the two regions

$$\delta_{\text{B.L.}} \sim \frac{v}{x_c}\,, \tag{D8}$$

which is increasingly narrow for $x_c \gg \sqrt{v}$. Similarly, we can verify that the mutation term M is negligible at $x = x_c$ as long as

$$x_c^2 \gg U_b \int ds\, \rho(s) s\,. \tag{D9}$$

It is clear that as we move toward even smaller fitnesses, Eq. (D5) must eventually break down, because it makes the nonsensical prediction that $w(x)$ increases for increasingly lower fitness when $x < 0$. At some intermediate point, the mutation term becomes relevant again, and the approximate differential equation becomes much more difficult to solve. Fortunately, as long as $x_c \gg \sqrt{v}$, the fixation probabilities for these fitnesses will be so low in this regime that we can effectively approximate them by $w(x) \approx 0$. In addition, we show in Appendix G that the dominant contribution from $w(x)$ comes from $x \approx x_c$, so our results will be insensitive to the form of $w(x)$ in this region for the moderate mutation rates considered here.

Putting everything together, we arrive at an approximate expression for the fixation probability,

$$w(x) \approx \begin{cases} 0 & \text{if } x < 0, \\ x_c e^{\frac{x^2 - x_c^2}{2v}} & \text{if } 0 < x < x_c, \\ x & \text{if } x > x_c. \end{cases} \tag{D10}$$

Note that while we have taken advantage of a sharp transition at $x = x_c$, we have not yet determined the value of x_c. Strictly speaking, the location of the transition point is completely determined by Eq. (D1), but in our approximate analysis, the delicate balance that determines this transition is overshadowed by the terms in the dominant balance. In order to tease out this dependence, we multiply both sides of Eq. (D1) by the Gaussian integrating factor $e^{-x^2/2v}$ and integrate over the relative fitness x. After an integration by parts, this has the effect of removing the "Gaussian" V and S terms and leaves us with the relation

$$\int_{-\infty}^{\infty} dx\, e^{-\frac{x^2}{2v}} w(x)^2 = U_b \int_{-\infty}^{\infty} dx\, w(x) \int_0^\infty ds\, \rho(s) \left[e^{-\frac{(x-s)^2}{2v}} - e^{-\frac{x^2}{2v}} \right]. \tag{D11}$$

We can now evaluate these integrals by using the approximate form of $w(x)$ given in Eq. (D10). The left hand side can be evaluated by splitting the region of integration into two pieces and using Laplace's approximation on each one:

$$\begin{aligned}\int_{-\infty}^{\infty} dx\, e^{-\frac{x^2}{2v}} w(x)^2 &= \int_{-\infty}^{0} 0 + \int_0^{x_c} dx\, A^2 e^{\frac{x^2}{2v}} + \int_{x_c}^{\infty} dx\, x^2 e^{-\frac{x^2}{2v}} \\ &= 0 + A^2 \frac{v}{x_c} e^{\frac{x_c^2}{2v}} + \frac{v}{x_c} x_c^2 e^{-\frac{x_c^2}{2v}} \\ &= 2Av\,, \end{aligned} \tag{D12}$$

where we have once again assumed that $x_c \gg \sqrt{v}$. The right hand side can evaluated in a similar manner:

$$\begin{aligned}\int dx\, e^{-\frac{x^2}{2v}} M = U_b \int_0^{x_c} dx\, A e^{\frac{x^2}{2v}} \int_0^{\infty} ds\, \rho(s) e^{-\frac{(x-s)^2}{2v}} + U_b \int_{x_c}^{\infty} dx\, x \int_0^{\infty} ds\, \rho(s) e^{-\frac{(x-s)^2}{2v}} \\ - U_b \int_0^{x_c} dx\, A - U_b \int_{x_c}^{\infty} dx\, x e^{-\frac{x^2}{2v}} \\ = vAU_b \left[\int ds\, \rho(s) e^{-\frac{s^2}{2v}} \left(\frac{e^{\frac{x_c}{v}s} - 1}{s} \right) + \int_{x_c}^{\infty} \frac{dx\, x}{vA} e^{-\frac{x^2}{2v}} \int_0^{\infty} ds\, \rho(s) e^{-\frac{s^2}{2v} + \frac{x_c}{v}s} \right. \\ \left. - \frac{1}{x_c} \left(1 + \frac{x_c^2}{v} \right) \right]. \end{aligned} \tag{D13}$$

Combining this with the LHS result, we find that the location x_c of the transition must obey the condition

$$2 = U_b \left[\int ds\, \rho(s) e^{-\frac{s^2}{2v}} \left(\frac{e^{\frac{x_c}{v}s} - 1}{s} \right) + \int_{x_c}^{\infty} \frac{dx}{v} \frac{x}{x_c} e^{\frac{x_c^2 - x^2}{2v}} \int_0^{\infty} ds\, \rho(s) e^{-\frac{s^2}{2v} + \frac{x}{v}s} - \left(\frac{1}{x_c} + \frac{x_c^2}{v} \right) \right]. \tag{D14}$$

The corresponding Eq. (10) in the main text is obtained by dropping the last term on the right, which is negligible when $x_c \gg \sqrt{v}$ because the first term effectively scales like $\exp(x_c^2/v)$.

APPENDIX E: EXPONENTIAL DISTRIBUTION

In this section, we implement our approximate analytical framework for the case where $\rho(s)$ is given by an exponential distribution

$$\rho(s) = \frac{1}{\sigma} e^{-s/\sigma}\,. \tag{E1}$$

1. Location of the transition

In order to carry out the integration over s in Eq. (D14), we notice that the integrands are dominated by an exponential factor whose argument is given by the function

$$g(s) = -\frac{s^2}{2v} + \frac{x}{v}s - \frac{s}{\sigma}\,, \tag{E2}$$

which suggests that they can be evaluated using Laplace's method. This function has a maximum when $s^* = x - \frac{v}{\sigma}$, and at this maximum point we find that

$$g(s^*) = \frac{(x - \frac{v}{\sigma})^2}{2v}\,, \quad g''(s^*) = -\frac{1}{v}\,. \tag{E3}$$

If we assume that $x_c - v/\sigma \gg \sqrt{v}$, then a simple application of Laplace's method reduces Eq. (D14) to the form

$$\begin{aligned} 2 &= \left[\frac{U_b}{\sigma} \frac{\sqrt{2\pi v}}{x_c - \frac{v}{\sigma}} e^{\frac{(x_c - \frac{v}{\sigma})^2}{2v}} \right] + \frac{U_b}{\sigma} \sqrt{2\pi v} e^{\frac{v}{2\sigma^2}} \int_{x_c}^{\infty} \frac{dx\, x}{vA} e^{-\frac{x}{\sigma}} \\ &= \frac{U_b}{\sigma} \frac{\sqrt{2\pi v}}{x_c - \frac{v}{\sigma}} e^{\frac{(x_c - \frac{v}{\sigma})^2}{2v}} + \frac{U_b}{v} \sqrt{2\pi v} \left(1 + \frac{\sigma}{x_c} \right) e^{\frac{(x_c - \frac{v}{\sigma})^2}{2v}}\,, \end{aligned} \tag{E4}$$

or

$$2 = \frac{U_b}{\sigma} \sqrt{2\pi v} \left[\frac{1}{x_c - \frac{v}{\sigma}} + \frac{\sigma}{v} \left(1 + \frac{\sigma}{x_c} \right) \right] e^{\frac{(x_c - \frac{v}{\sigma})^2}{2v}}\,. \tag{E5}$$

2. Consistency condition for the velocity

In order to self-consistently solve for the velocity, we substitute our approximate expressions for the fixation probability Eq. (D10) and the fitness profile Eq. (A1) into the velocity consistency condition in the main text and evaluate the s-integrals using Laplace's method. This yields

$$\begin{aligned} v &= NU_b \int_0^\infty ds\, s\rho(s) \int_{-\infty}^\infty dx\, w(x) f(x-s) \\ &= \frac{NU_b}{\sqrt{2\pi v}} \left[\int_0^\infty ds \left(\frac{s}{\sigma}\right) e^{-\frac{s}{\sigma}-\frac{s^2}{2v}} \int_0^{x_c} dx\, A e^{\frac{s}{v}x} + \int_{x_c}^\infty dx\, x e^{-\frac{x^2}{2v}} \int_0^\infty ds \left(\frac{s}{\sigma}\right) e^{\frac{x}{v}s - \frac{s^2}{2v} - \frac{s}{\sigma}} \right] \\ &= \frac{NU_b}{\sqrt{2\pi v}} \left[\frac{vA}{\sigma}\sqrt{2\pi v} e^{\frac{(x_c - \frac{v}{\sigma})^2}{2v}} + \frac{\sqrt{2\pi v}}{\sigma} e^{\frac{v}{2\sigma^2}} \left[\sigma e^{-\frac{x_c}{\sigma}} \left(x_c^2 - \frac{v}{\sigma}(x_c+\sigma) + 2x_c\sigma + 2\sigma^2 \right) \right] \right], \end{aligned} \tag{E6}$$

or

$$1 = NU_b \frac{x_c^2}{v} \left[1 - \frac{v}{x_c^2} + \frac{2\sigma}{x_c} + \frac{2\sigma^2}{x_c^2} \right] e^{-\frac{x_c}{\sigma} + \frac{v}{2\sigma^2}}. \tag{E7}$$

Together, Eq. (E7) and Eq. (E5) allow us to solve for v and x_c.

APPENDIX F: GENERAL DISTRIBUTIONS

We now consider a broader class of distributions $\rho(s)$ that result in a $\rho_f(s)$ that is strongly peaked around a characteristic effect size (exact technical conditions are defined below). This will tend to be the case for most unimodal $\rho(s)$ with exponentially bounded tails.

1. Location of the transition

In general, the s-integrals in Eq. (D14) involve an exponential factor whose argument is the function

$$g(s) = -\frac{s^2}{2v} + \frac{x}{v}s + \log \rho(s), \tag{F1}$$

which has a maximum s^* determined by

$$g'(s^*) = -\frac{s^*}{v} + \frac{x^*}{v} + \frac{\partial \log \rho(s^*)}{\partial s} = 0, \tag{F2}$$

and a characteristic width

$$\Delta = |g''(s^*)|^{-1/2} = \left[\frac{1}{v} - \frac{\partial^2 \log \rho(s^*)}{\partial s^2} \right]^{-1/2}. \tag{F3}$$

If $s^* \gg \Delta$ and $x_c s^* \ll v$, we can compute the s-integrals in Eq. (D14) using a Laplace approximation, which yields

$$2 = U_b \left[\frac{\sqrt{2\pi\Delta^2} e^{g(s^*)}}{s^*} + \int_{x_c}^\infty \frac{dx}{v} \frac{x}{v} \sqrt{2\pi\Delta^2} e^{\frac{x_c^2}{2v} - \frac{x^2}{2v} + g(s^*)} \right]. \tag{F4}$$

If $\frac{x_c - s^*}{\sqrt{v}} \gg 1$, we can exmploy the Laplace approximation again on the x-integral, and we obtain

$$2 = \frac{U_b \sqrt{2\pi\Delta^2} \rho(s^*)}{s^*} \left[1 - \frac{s^*}{x_c} \right]^{-1} e^{\frac{x_c s^*}{v} - \frac{s^{*2}}{2v}}. \tag{F5}$$

This expression will apply for all distributions that satisfy the required conditions for the approximations:

$$\frac{s^*}{\Delta} \gg 1, \tag{F6}$$

$$\frac{x_c s^*}{v} \gg 1, \tag{F7}$$

$$\frac{x_c - s^*}{\sqrt{v}} \gg 1, \tag{F8}$$

in addition to the assumption that $x_c \gg \sqrt{v}$, which is required for Eq. (D10) to hold. In other words, the dominant effect size must be greater than the typical width of $\rho_f(s)$ as well as the typical width of the boundary layer $\delta_{B.L.} \sim v/x_c$, while the optimal background fitness must be several standard deviations away from the mean of $f(x)$.

For concreteness, we apply this analysis to the class of "exponential-like" distributions of the form

$$\rho(s) = \frac{1}{\sigma\Gamma(1+\beta^{-1})} e^{-\left(\frac{s}{\sigma}\right)^{\beta}}, \tag{F9}$$

with $\beta \geq 1$. When $\beta \gg 1$, the characteristic effect size is given by the self-consistent solution

$$s^* \approx \left(\frac{x_c\sigma^\beta}{\beta v}\right)^{\frac{1}{\beta-1}} \left[1 - \frac{1}{1+\beta(\beta-1)\frac{v}{\sigma^2}\left(\frac{x_c}{\beta v}\right)^{\frac{\beta-2}{\beta-1}}}\right] \approx \left(\frac{x_c\sigma^\beta}{\beta v}\right)^{\frac{1}{\beta-1}}, \tag{F10}$$

which requires that $s^* \ll x_c$. The characteristic width Δ is therefore given by

$$\Delta = \left[\frac{1}{v} + \frac{\beta(\beta-1)}{\sigma^2}\left(\frac{s^*}{\sigma}\right)^{\beta-2}\right]^{-1/2} \approx \frac{\sigma}{\sqrt{\beta(\beta-1)\left(\frac{x_c\sigma}{\beta v}\right)^{\frac{\beta-2}{\beta-1}}}}. \tag{F11}$$

On the other hand, when $\beta = 1$, we have $s^* = x_c - v/\sigma$ and the characteristic width is given by $\Delta = v$, so we recover Eq. (E5) with a slight loss in accuracy.

2. Consistency condition for the velocity

We can obtain the second relation between v and x_c in the same manner that we did for the exponential case, by substituting our approximate expressions for $w(x)$ and $f(x)$ into the consistency condition in the main text. In this case, however, we can take a short-cut (with the same accuracy as the Laplace approximations above) by noting that

$$v = NU_b \int_{-\infty}^{\infty} dx\, w(x) \int_0^{\infty} ds\, s\rho(s) f(x-s) \approx \frac{Ns^*}{\sqrt{2\pi v}} \int_{-\infty}^{\infty} dx e^{-\frac{x^2}{2v}} M \approx \frac{2Ns^* v x_c e^{-\frac{x_c^2}{2v}}}{\sqrt{2\pi v}}, \tag{F12}$$

or

$$1 = \frac{2Ns^* x_c}{\sqrt{2\pi v}} e^{-\frac{x_c^2}{2v}}. \tag{F13}$$

Multiplying Eqs. (F13) and (F5), we obtain an expression more similar to its exponential analog in Eq. (E7):

$$1 = \frac{NU_b\sqrt{2\pi\Delta^2}\rho(s^*)x_c}{\sqrt{2\pi v}} \left[1 - \frac{s^*}{x_c}\right]^{-1} e^{-\frac{(x_c-s^*)^2}{2v}}. \tag{F14}$$

Together, Eqs. (F5) and (F14) allow us to solve for v and x_c.

APPENDIX G: STATISTICS OF FIXED MUTATIONS

In the main text, we have seen how our expressions for $w(x)$ and $f(x)$ can be combined to determine the distribution of fixed mutations, $\rho_f(s)$. This procedure can be generalized to include other statistics of successful mutations. In general, we can associate three quantities with every mutation: its fitness effect (s), the relative fitness of the background in which it arose (x_i), and the relative fitness of the mutant immediately after the mutation event (x_f). Let $p(x_i, s, x_f|\text{fixed})$ denote the joint distribution of these quantities conditioned on successful fixation. Then from Bayes' theorem, we have

$$p(x_i, s, x_f|\text{fixed}) \propto p(\text{fixed}|x_i, s, x_f)p(x_i, s, x_f) \tag{G1}$$

$$\propto w(x_f)f(x_i)\rho(s)\delta(x_f - x_i - s), \tag{G2}$$

which, in principle, allows us to calculate any derived statistic.

For instance, we can use this joint distribution to calculate the joint MLE – the most likely x_i, s, and x_f given that the mutation fixed. Since the three quantities are connected by the δ-function, it is easiest to do this calculation after integrating over x_i and then substituting $x_i = x_f - s$ at the end. We therefore try to maximize

$$p(s, x_f|\text{fixed}) \propto w(x_f) f(x_f - s)\rho(s) \tag{G3}$$

$$\propto \begin{cases} \exp\left(\log x_f - \frac{(x_f-s)^2}{2v} + \log\rho(s)\right) & \text{if } x_f > x_c, \\ \exp\left(\frac{x_f^2}{2v} - \frac{(x_f-s)^2}{2v} + \log\rho(s)\right) & \text{if } x_f < x_c. \end{cases} \tag{G4}$$

Since we already assumed that $x_c \gg \sqrt{v}$, this function is maximized when $x_f = x_c$ and s satisfies

$$-\frac{s}{v} + \frac{x_c}{v} + \partial_s \log\rho(s) = 0\,, \tag{G5}$$

which is exactly the definition of s^* from the main text. We therefore have for the joint MLEs:

$$\hat{x}_i = x_c - s^*\,, \tag{G6}$$

$$\hat{s} = s^*\,, \tag{G7}$$

$$\hat{x}_f = x_c\,. \tag{G8}$$

APPENDIX H: SINGLE-s EQUIVALENCE

Previous work on adaptation in large asexual populations often assumes (either implicitly or explicitly) a type of "equivalence principle," in which the dynamics of adaptation under an arbitrary distribution $\rho(s)$ can be mapped to an equivalent model with a single, *effective*[2] selection coefficient s_{eff} and mutation rate U_{eff} [11, 12]. This assumption is motivated by the intuition that mutations with $s < s_{\text{eff}}$ will tend to be lost to interference with stronger mutations, while those with $s > s_{\text{eff}}$ will typically be too rare to occur before a fitter multiple mutant establishes.

In addition to offering an intuitive picture of the effects of interference on the dynamics of adaptation, this idea of single-s equivalence can have important consequences for experimental measurement and model building. If a "strong" form of the equivalence principle holds, and *all* observable quantities are equivalent to an effective model with the same effective parameters, it would severely limit our power to infer the underlying distribution $\rho(s)$ by measuring these quantities for a particular population size. On the other hand, a strong equivalence principle implies that more complicated models (e.g. those including recombination, deleterious mutations, epistasis, etc.) could be safely constructed from single-s theories without sacrificing realism, as long as we are careful to recognize that s_{eff} and U_{eff} themselves depend on the population parameters $(N, U_b, \rho(s))$ in a potentially complicated way. This last point is an important one, since it implies that even if single-s equivalence holds, the functional dependence of v on N (or any other population parameter) is *not* the same as a "true" single-s model where s_{eff} is independent of N. This difference in scaling is already an important difference from a true single-s theory, and may offer a means to distinguish between different underlying distributions by measuring the rates of adaptation at different population sizes.

It may also be the case that a much weaker form of the equivalence principle is true, in which each aspect of the dynamics (e.g. steady-state rates of adaptation, transient effects, fluctuations, neutral diversity, etc.) is described by a *different* effective model. In this case, the utility of the principle is reduced, since the equivalent model must be established for each quantity of interest. Previous studies have almost exclusively focused on the concept of equivalence for the steady-state rate of adaptation. We consider this case as well, and extend this weaker form of the equivalence principle to include the dominant mutant fitness x_c. (In our approximate framework, since $w(x)$ depends on $\rho(s)$ only through v and x_c, this weak equivalence extends to the entire function $w(x)$ as well.) Further generalization of these ideas for other quantities remains an important avenue for future work.

In order to establish a mapping to a model with a single selection coefficient, we must first introduce a theory of single-s models in the multiple-mutation regime. Several examples already exist in the literature, but we will find it most convenient to apply the approach outlined above to the case where

$$\rho(s) = \delta(s - s_{\text{eff}})\,, \tag{H1}$$

---

[2] We use the term *effective parameter* to denote a parameter that is itself a function of the underlying parameters $(N, U_b, \rho(s))$

and $U_b = U_{\text{eff}}$. Under the usual assumptions that $x_c - s_{\text{eff}} \gg \sqrt{v}$ and $x_c s_{\text{eff}}/v \gg 1$, Eq. (D14) reduces to

$$2 = \frac{U_{\text{eff}}}{s_{\text{eff}}}\left[1 - \frac{s_{\text{eff}}}{x_c}\right]^{-1} e^{\frac{x_c s_{\text{eff}}}{v} - \frac{s_{\text{eff}}^2}{2v}}, \tag{H2}$$

and the consistency condition for the velocity becomes

$$1 = \frac{NU_{\text{eff}} x_c}{\sqrt{2\pi v}}\left[1 - \frac{s_{\text{eff}}}{x_c}\right]^{-1} e^{-\frac{(x_c - s_{\text{eff}})^2}{2v}}. \tag{H3}$$

By definition, v and x_c must be the same in this equivalent model. Since our approximate expression for $w(x)$ in Eq. (D10) depends only on these two quantities, it will also be identical at leading order. We obtain the desired mapping by comparing Eqs. (H2) and (H3) with their counterparts for the full $\rho(s)$ in Eqs. (F5) and (F14) and solving for s_{eff} and U_{eff}. We immediately see that this equivalence holds if and only if

$$s_{\text{eff}} = s^*, \quad U_{\text{eff}} = U_b\sqrt{2\pi\Delta^2}\rho(s^*). \tag{H4}$$

Thus, the effective selection coefficient has an intuitive interpretation as the peak of $\rho_f(s)$ (or rather, the joint MLE identified in Appendix G) and the effective mutation rate is rescaled by the probability of observing a mutation of that size under the original distribution. This novel prediction shows that our effective theory is more than a mathematical nicety, but that it is related to the "relevant" effect sizes identified by $\rho_f(s)$. Furthermore, we see that the form of the single-s mapping to s_{eff} and U_{eff} is essentially the same for a wide class of $\rho(s)$.

In the special case where $s^* \approx x_c$, it can be instructive to consider an even simpler alternative mapping. This will occur, for example, in the intermediate-NU_b exponential regime where the typical mutational effect is on the order of the width of the fitness profile. In this case, we can gain additional intuition about the dynamics of adaptation by mapping to a selective-sweeps single-s theory in which only one driving mutation is typically competing at a given time. Using the well-known formula

$$v = NU_{\text{eff}} s_{\text{eff}}^2 \tag{H5}$$

for the rate of adaptation in this regime, we see that our equivalence holds if we take

$$(NU)_{\text{eff}} = \left[N\frac{v}{x_c - s^*} f(x_c - s^*)\right]\left[U_b\sqrt{2\pi\Delta^2}\rho(s^*)\right]. \tag{H6}$$

Since the population size and mutation rate always enter together in the selective-sweeps regime, we can never entirely decompose these two parameters, but we can understand Eq. (H6) more intuitively if we take U_{eff} to be same as in Eq. (H4) and define an *effective population size*

$$N_{\text{eff}} = N\left(\frac{v}{x_c - s^*}\right) f(x_c - s^*), \tag{H7}$$

where $x_c - s^*$ is the most likely background fitness identified in Appendix G. Again, we find that our effective parameter has an intuitive interpretation: in this case, the effective population size is scaled by the probability of a given mutation arising on the most likely background fitness, as determined by the full dynamics.

The dramatic difference in the equivalent single-s model reflects a dramatic difference in the dynamics of fixation in these two regimes. The typical mutations in the intermediate-NU_b exponential regime are sufficiently large that they often fix in the linear (Haldane) region of $\pi(s)$, which implies that they are relatively free from interference effects. In contrast, the typical mutations in the large-NU_b exponential regime (and the $\beta > 1$ distributions above) are much smaller compared to the width of $f(x)$, so the background on which they arise plays a much larger role in their ultimate chances of fixation.

The fact that an exponential $\rho(s)$ maps to a selective sweeps model in certain regimes explains why the intuitive calculation of Desai and Fisher [1] did not succeed in this case, since they exclusively looked for a mapping to the multiple-mutations regime. In addition, it may explain why the original theories of clonal interference were much more successful in predicting the rate of adaptation for exponential $\rho(s)$, and why numerical "driving mutation" approximations [13] were able to correct for the discrepancy in $\rho_f(s)$.

APPENDIX I: SIMULATIONS AND NUMERICAL METHODS

We validate several of our key approximations in the main text by comparing our theoretical predictions with the results of foward-time, discrete-generation simulations similar to the standard Wright-Fisher model [14]. These simulations begin with a clonal population of N individuals, and in each subsequent generation the population undergoes a selection step followed by a mutation step. In the selection step, each lineage (i.e. unique genotype) is assigned a new size from a Poisson distribution with mean

$$\lambda_i = C(1 + x_i)n_i \,, \tag{I1}$$

where n_i is the current size of the lineage, x_i is its fitness relative to the population average, and $C = N/\sum_i n_i$ is a normalization constant chosen to ensure that the total population size remains close to N. In the mutation step, each individual mutates with probability U_b, in which case it founds a new lineage with a fitness increment randomly drawn from $\rho(s)$. This process is continued for a sufficiently long period of time that the population reaches the steady-state mutation-selection balance introduced in the main text.

For the relatively large population sizes considered in this work, this simulation algorithm is virtually indistinguishable from standard Wright-Fisher dynamics. In particular, it shares the property that the variance in the number of offspring differs from that of the continuous-time branching process by a factor of $c = 2$ [1]. Like the $c = 1/2$ factor arising in the tunable constraint framework of Appendix C, we can account for this difference simply by making the replacement $N \to cN$ in the theoretical expressions derived in the main text.

The numerical values for our theoretical predictions used in the figures are obtained by numerically solving the system of transcendental equations for v and x_c given in Appendix E and Appendix F for the exponential and $\beta > 1$ distributions. This can be done using standard iterative root-finding procedures such as the `fsolve()` function in the SciPy Python library [15]. To ensure proper convergence, care must be taken to choose a suitable "guess" for the root, which we take to be equal to our approximate solution for v in the main text (a similar expression can be easily derived for x_c). This generally leads to good convergence in the parameter regimes we tested, but extension to additional parameter regimes may require more fine-tuning of the algorithm. A copy of our implementation in Python is freely available upon request.

[1] M. M. Desai and D. S. Fisher, "Beneficial mutation selection balance and the effect of genetic linkage on positive selection," *Genetics*, vol. 176, pp. 1759–1798, 2007.

[2] I. M. Rouzine, J. Wakeley, and J. M. Coffin, "The solitary wave of asexual evolution," *Proc. Natl. Acad. Sci. USA*, vol. 100, pp. 587–592, 2003.

[3] I. M. Rouzine and J. M. Coffin, "Evolution of hiv under selection and weak recombination," *Genetics*, vol. 170, pp. 7–18, 2005.

[4] R. Neher, B. I. Shraiman, and D. S. Fisher, "Rate of adaptation in large sexual populations," *Genetics*, vol. 184, pp. 467–481, 2010.

[5] I. Rouzine, E. Brunet, and C. Wilke, "The traveling-wave approach to asexual evolution: Muller's ratchet and the speed of adaptation," *Theor Pop Bio*, vol. 73, pp. 24–46, 2008.

[6] I. M. Rouzine and J. M. Coffin, "Many-site adaptation in the presence of infrequent recombination," *Theor Pop Bio*, vol. 77, pp. 189–204, 2010.

[7] E. Brunet, I. M. Rouzine, and C. O. Wilke, "The stochastic edge in adaptive evolution," *Genetics*, vol. 179, pp. 603–620, 2008.

[8] L. Tsimring, H. Levine, and D. Kessler, "Rna virus evolution via a fitness-space model," *Phys. Rev. Lett.*, vol. 90, p. 088103, 1996.

[9] O. Hallatschek, "The noisy edge of traveling waves," *Proc. Natl. Acad. Sci. USA*, vol. 108, pp. 1783–1787, 2011.

[10] J. Haldane, "The mathematical theory of natural and artificial selection, part v: selection and mutation," *Proc. Camb. Philos. Soc.*, vol. 23, pp. 828–844, 1927.

[11] M. Hegreness, N. Shoresh, D. Hartl, and R. Kishony, "An equivalence principle for the incorporation of favorable mutations in asexual populations," *Science*, vol. 311, pp. 1615–1617, 2006.

[12] M. M. Desai, D. S. Fisher, and A. W. Murray, "The speed of evolution and the maintenance of variation in asexual populations," *Curr. Biol.*, vol. 17, pp. 385–394, 2007.

[13] S. Schiffels, G. Szöllösi, V. Mustonen, and M. Lässig, "Emergent neutrality in adaptive asexual evolution," *Genetics*, vol. 189, pp. 1361–1375, 2011.

[14] W. J. Ewens, *Mathematical Population Genetics*. New York: Springer-Verlag, second ed., 2004.

[15] E. Jones, T. Oliphant, P. Peterson, *et al.*, "SciPy: Open source scientific tools for Python," 2001–.